

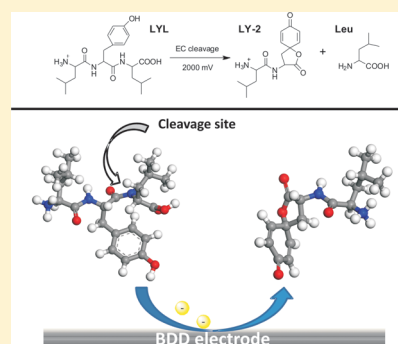
# Boron-Doped Diamond Electrodes for the Electrochemical Oxidation and Cleavage of Peptides

Julien Roeser, Niels F. A. Alting, Hjalmar P. Permentier, Andries P. Bruins, and Rainer Bischoff\*

Analytical Biochemistry and Mass Spectrometry Core Facility, Department of Pharmacy, University of Groningen, A. Deusinglaan 1, 9713 AV Groningen, The Netherlands

## Supporting Information

**ABSTRACT:** Electrochemical oxidation of peptides and proteins is traditionally performed on carbon-based electrodes. Adsorption caused by the affinity of hydrophobic and aromatic amino acids toward these surfaces leads to electrode fouling. We compared the performance of boron-doped diamond (BDD) and glassy carbon (GC) electrodes for the electrochemical oxidation and cleavage of peptides. An optimal working potential of 2000 mV was chosen to ensure oxidation of peptides on BDD by electron transfer processes only. Oxidation by electrogenerated OH radicals took place above 2500 mV on BDD, which is undesirable if cleavage of a peptide is to be achieved. BDD showed improved cleavage yield and reduced adsorption for a set of small peptides, some of which had been previously shown to undergo electrochemical cleavage C-terminal to tyrosine (Tyr) and tryptophan (Trp) on porous carbon electrodes. Repeated oxidation with BDD electrodes resulted in progressively lower conversion yields due to a change in surface termination. Cathodic pretreatment of BDD at a negative potential in an acidic environment successfully regenerated the electrode surface and allowed for repeatable reactions over extended periods of time. BDD electrodes are a promising alternative to GC electrodes in terms of reduced adsorption and fouling and the possibility to regenerate them for consistent high-yield electrochemical cleavage of peptides. The fact that OH-radicals can be produced by anodic oxidation of water at elevated positive potentials is an additional advantage as they allow another set of oxidative reactions in analogy to the Fenton reaction, thus widening the scope of electrochemistry in protein and peptide chemistry and analytics.



Carbon-based electrodes are widely used in electrochemistry and are often preferred to noble metal electrodes for oxidation of organic and biological molecules.<sup>1</sup> The main benefits of such materials are their electrocatalytic activity for a variety of redox reactions, their wide potential window, low cost, and the possibility of preparing porous materials with large surface areas (porous graphite carbon). Graphite and glassy carbon electrodes are, however, also known to suffer from surface fouling and from oxide formation by reaction with oxygen and water. These surface reactions can have a significant effect on adsorption, electron-transfer kinetics and electrocatalysis.<sup>2</sup>

The introduction of diamond-based materials as electrodes in the late 1980s by Pleskov et al.<sup>3</sup> was a major advance in electrochemistry. Natural diamond is an electrically insulating material that cannot be used as an electrode but the introduction of impurities within the  $sp^3$ -hybridized tetrahedral lattice of diamond makes it conductive. Boron is by far the most widely used dopant and yields p-type semiconductors or materials with metal-like electronic properties depending on the doping levels.<sup>4</sup> Boron-doped diamond (BDD) thin-films are mostly prepared by chemical vapor deposition (CVD) on silicon or metallic substrates under a hydrogen atmosphere yielding H-terminated surfaces. Preparation techniques, characterization, surface modifications, and electrochemical properties of BDD electrodes have been reviewed elsewhere.<sup>1,2,4-8</sup>

BDD electrodes have become attractive materials for electrochemical applications in place of glassy carbon or graphite due to their wider potential window, low background currents, higher chemical inertness, high thermal conductivity, and high mechanical stability. The high overpotential for both oxygen and hydrogen evolution are responsible for the wide potential window (the widest so far measured in aqueous electrolytes) and allows conversion of molecules with high oxidation and reduction potentials. Chemical inertness and low background currents stem from the  $C-sp^3$  hybridization of diamond which has a low capacitance and prevents surface oxide formation.<sup>1</sup> Owing to these properties, BDD is a material well-known for its low adsorption, resistance to (bio)fouling, excellent response stability, and high current signal-to-noise ratio which made it popular for a wide range of electroanalytical applications for both inorganic and organic compounds.<sup>4,8</sup>

Electrochemical properties and performance of BDD electrodes depend on several factors such as doping levels, nondiamond impurities ( $C-sp^2$  carbon) and surface termination (hydrogen or oxygen). The latter has a great influence on charge transfer rates at the electrode surface which decrease

Received: December 30, 2012

Accepted: June 12, 2013

upon the gradual replacement of superficial hydrogen by oxygen-terminated sites during repeated anodic oxidation or prolonged exposure to ambient air.<sup>9,10</sup> BDD electrode pretreatment methods at high anodic or cathodic potentials in an acidic environment were shown to allow tuning of surface termination states in order to study reaction kinetics.<sup>10,11</sup> Both anodic and cathodic pretreatment may improve the voltammetric response of analytes (ref 11 and references therein). Cathodic pretreatment can for instance be used for the regeneration of an electrode surface that was passivated due to analyte adsorption on an O-terminated surface, as has been shown in the context of the electrochemical oxidation of proteins.<sup>12</sup>

Anodic hydroxyl radical production by oxidation of water can occur very effectively on BDD electrodes due to the high overpotential for oxygen evolution. Hydroxyl radical generation at BDD electrodes is very specific for this material and is widely used for water treatment and destruction of organic or inorganic pollutants, which is by far the most investigated application area for BDD electrodes. Formation of hydroxyl radicals and even methoxy radicals has also been applied to other fields such as protein footprinting<sup>13</sup> and organic synthesis.<sup>14–16</sup>

Electrochemical oxidation of peptides and proteins has been shown to yield specific cleavage of the peptide bonds C-terminal to Tyr and Trp residues and holds promise to become an instrumental alternative to chemical and enzymatic protein cleavage.<sup>17–19</sup> Electrochemical cleavage has so far mainly been carried out on purely carbon-based materials. Adsorption and fouling of carbon electrodes are aggravating issues when working with large (bio)molecules and impair repeatability and reproducibility, or even prevent oxidation to occur at all.<sup>18</sup> Moreover, Tyr dimer formation by cross-linking reactions<sup>20,21</sup> occurs on carbon-based materials<sup>22</sup> due to strong affinity and adsorption of the phenolic ring to the electrode surface.<sup>23</sup> Such drawbacks contribute to the limited cleavage yields. BDD is thus a promising electrode material for electrochemical oxidation of peptides and proteins, owing to its limited adsorption. Studies involving a single amino acid or amino acid mixtures have shown improved performance for electrochemical detection in terms of lower adsorption and improved electrode stability, although in some cases fouling and electrode passivation have been observed when working with concentrated solutions in the millimolar range.<sup>24–30</sup> BDD electrodes have also been investigated for the electrochemical detection of peptides and proteins (both metallo- and nonmetal-containing proteins)<sup>12,31–38</sup> and for studies on resistance to protein fouling.<sup>39–42</sup>

We report here the first comparison and evaluation of the performance of BDD versus GC electrodes for the electrochemical oxidation and cleavage of peptides. Products were monitored by LC–MS which provided detailed information about the reactions occurring at the electrode surfaces. The potential regions of the two different oxidation mechanisms occurring on BDD electrodes, i.e. direct electron transfer processes and hydroxyl radical formation, were investigated as well as methods to regenerate the electrode surface after performance loss upon prolonged oxidation experiments.

## ■ EXPERIMENTAL SECTION

**Chemicals.** The tripeptides LYL, LWL and LFL were obtained from Research Plus Inc. (Barnegat, NJ, USA). Angiotensin I (DRVYIHPFHL), Adrenocorticotrophic hormone

(ACTH) 1–10 (SYSMEHFRWG) and formic acid (HCOOH) were purchased from Sigma-Aldrich (Steinheim, Germany). Water was purified by an Arium Ultrapure water system (conductivity 18.2 MΩ.cm, Sartorius Stedim Biotech, Göttingen, Germany). HPLC supra gradient acetonitrile was purchased from Merck (Darmstadt, Germany).

**Electrochemical Oxidation of Peptides.** Stock solutions of LYL, LWL, LFL, angiotensin I, and ACTH 1-10 were prepared at a concentration of 1 mM in 90/10/1 (v/v/v) ultrapure water/acetonitrile/formic acid and diluted to a final concentration of 5 μM prior to oxidation.

The tripeptide solutions were oxidized with a Flexcell thin-layer cell (Antec Leyden, Leiden, The Netherlands) with Magic Diamond (BDD) and glassy carbon (GC) working electrodes (8 mm diameter, surface area of 50.3 mm<sup>2</sup>), and a palladium (Pd/H<sub>2</sub>) reference electrode (Hy-REF). Cathodic pretreatment of BDD electrodes was performed prior to all experiments at a constant potential of –3000 mV for 1 h in the presence of 0.5 M sulfuric acid in water at a flow rate of 5 μL/min. Prior to use, BDD electrodes were washed with methanol and ultrapure water. GC electrodes were polished using diamond spray (1 μm particles) and subsequently rinsed with ultrapure water.

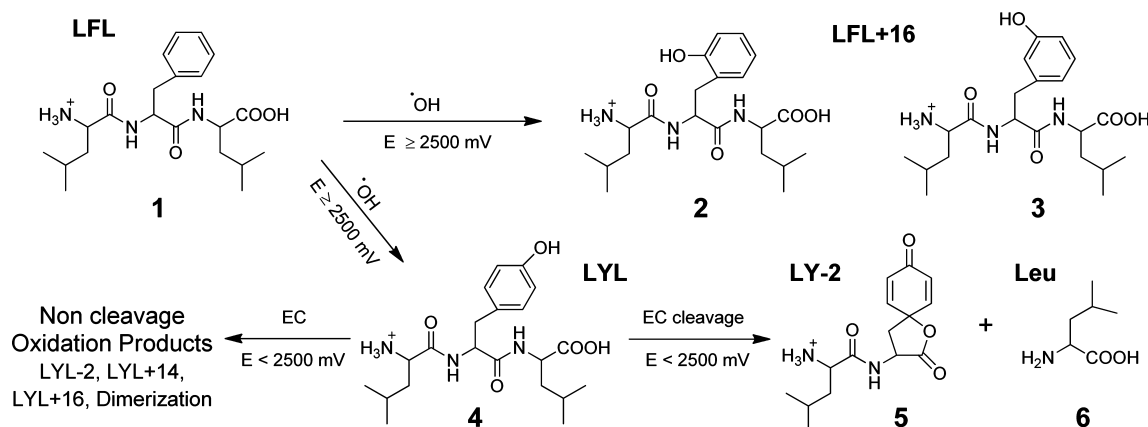
The potentials were controlled with a homemade potentiostat controlled by a MacLab system (ADInstruments, Castle Hill, NSW, Australia) and EChem software (eDAQ, Denistone East, NSW, Australia). The anodic currents obtained in the course of the experiments are reported in Table S3 in the Supporting Information (SI).

**Cyclic Voltammetry.** Cyclic voltammograms (CVs) were recorded with the thin-layer cell (Flexcell, Antec Leyden), with either a BDD or GC working electrode. The GC electrode was cleaned by polishing with diamond slurry according to the manufacturer's protocol. The BDD electrode was cleaned by cathodic pretreatment for 1 h at –3000 mV with 0.5 M sulphuric acid in water at a flow rate of 5 μL/min.

Samples with or without peptide in H<sub>2</sub>O/CH<sub>3</sub>CN/FA 89:10:1 were infused at 5 μL/min. Peptide concentration was 1 mM. The potentials were controlled with a homemade potentiostat controlled by a MacLab system (ADInstruments, Castle Hill, NSW, Australia) and EChem software (eDAQ, Denistone East, NSW, Australia). Ten consecutive CVs were recorded at a scan rate of 100 mV/s. For GC the potential range was from 0 to 2000 mV, for BDD from 0 to 3500 mV.

**Liquid Chromatography–Mass Spectrometry (LC–MS).** Liquid chromatography was performed on an Ultimate plus system (Dionex-LC Packings, Amsterdam, The Netherlands) equipped with an Ultimate gradient pump and Famos well plate Microautosampler. A Vydac RP-C<sub>18</sub> column (150 mm × 1 mm i.d., 5 μm particles, 300 Å pore size, Grace Vydac) was used for chromatographic separation at a flow rate of 50 μL/min. Mobile phase A consisted of ultrapure water with 0.1% formic acid. Mobile phase B was acetonitrile with 0.1% formic acid.

For analysis of the peptide-derived reaction products, 50 μL injections of the collected oxidized solutions were performed, and separation was achieved with a gradient of B (5–50% at 1%/min). The column was directly coupled to an API365 triple quadrupole mass spectrometer (AB-Sciex, Concord, Ontario, Canada) upgraded to EP10+ (Ionics, Bolton, Ontario, Canada) and equipped with a TurboIonSpray source for product detection in the positive ion mode.

Scheme 1. Hydroxyl-Radical-Induced Oxidation of the Tripeptide LFL on BDD electrodes<sup>a</sup>

<sup>a</sup>Para-hydroxylation of LFL yields the tripeptide LYL which can undergo further direct electron transfer reactions including cleavage of the peptide bond C-terminal to Tyr.

## RESULTS AND DISCUSSION

**Direct Oxidation vs Electrochemical Hydroxyl Radical Formation.** The high overpotential for oxygen evolution on BDD electrodes allows efficient anodic oxidation of water to hydroxyl radicals. Generation of hydroxyl radicals on BDD electrodes takes place at elevated potentials which can vary from one electrode to another, depending on the physical, chemical, and electronic properties of the material as was observed when comparing BDD electrodes from different manufacturers. Experiments performed with a similar thin-layer cell (5040 cell, ESA Inc., Bedford, MA, U.S.A.) showed that less positive potentials were required to generate hydroxyl radicals on a BDD electrode compared to the Antec thin-layer cells used in the present study. We presume that the difference of potential between the two systems stems from the different doping levels of the BDD electrodes (the latter information is not known to us).

The tripeptide LFL (**1**) (Scheme 1) was used to determine the potential limit at which hydroxyl radicals are generated in our system, since the aromatic ring of phenylalanine (Phe) cannot undergo direct oxidation by electron transfer reactions but is also a target for hydroxylation by reactive oxygen species.<sup>5</sup> Parts A and B of Figure 1 compare the base peak chromatograms obtained after oxidation of LFL (**1**) at a BDD electrode at 2000 mV and 2500 mV vs Pd/H<sub>2</sub>. The formation of hydroxyl radicals by oxidation of water occurred at 2500 mV as indicated by the presence of LFL oxidation products eluting prior to the unoxidized tripeptide in LC–MS (Figure 1B). The combined extracted ion chromatograms in Figure 1C illustrate in more detail the range of products obtained for LFL (**1**) at 2500 mV. The presence of products with a mass increase of 16 Da (*m/z* 408) compared to LFL (*m/z* 392) indicates the formation of hydroxylated LFL that occurs via hydroxyl radical attack. Despite their broad range of reactivity, hydroxyl radicals preferably target oxidation-sensitive amino acid side chains (i.e., Cys, Met, Trp, Tyr, Phe, and His) within peptides and proteins.<sup>5,43</sup> The presence of three peaks with a mass increment of 16 Da suggests that oxidation in the ortho-, meta-, and para-positions of the aromatic ring occurred, yielding hydroxylated LFL (**2**), (**3**), and (**4**), respectively (Scheme 1). The high peak intensities of LFL+32 Da products, also eluting as three chromatographic peaks, show that a second hydroxylation step is favored under these conditions. This secondary oxidation

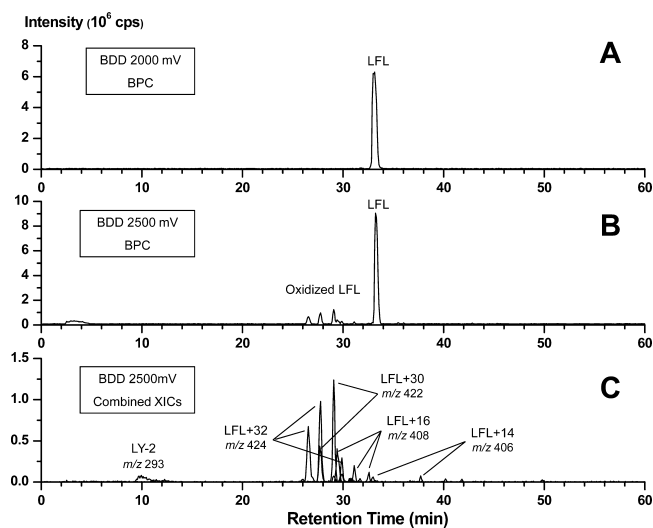


**Figure 1.** LC–MS chromatograms of reaction products obtained after oxidation of 5  $\mu\text{M}$  LFL in H<sub>2</sub>O/CH<sub>3</sub>CN/HCOOH (89:10:1) at a flow rate of 5  $\mu\text{L}/\text{min}$  on a BDD electrode. Base-peak chromatograms (BPC) obtained after oxidation at (A) 2000 mV and (B) 2500 mV. (C) Extracted ion chromatograms (XICs) of the oxidation products obtained at 2500 mV.

step can occur via two different mechanisms: a second hydroxyl radical attack or direct electrochemical oxidation of hydroxylated LFL. Indeed, hydroxylation of Phe in the para-position leads to the formation of Tyr and in this case the formation of the tripeptide LYL (**4**), which can react further by direct electron transfer reactions. As described in previous work<sup>19</sup> and shown in Scheme 1, LYL (**4**) can undergo dehydrogenation, hydroxylation, or a combination of those reactions yielding products with a mass decrease of 2 Da or a mass increase of 16 and 14 Da, respectively. These products are all observed in Figure 1C and are labeled LFL+14, LFL+32, and LFL+30, respectively. Finally, cleavage of the peptide bond next to Tyr by direct electrochemical oxidation followed by a secondary hydrolysis step<sup>19</sup> yielding the dipeptide LY-2 (**5**) occurs as well as shown by the presence of the early eluting *m/z* 293 product (Figure 1C).

Oxidation products of LFL were absent at 2000 mV (Figure 1A). Therefore, anodic oxidation of water leading to the

formation of hydroxyl radicals did not occur at 2000 mV, making this potential suitable when only direct electrochemical oxidation reactions are desired, such as the electrochemical peptide cleavage C-terminal to Tyr or Trp.

**Cathodic Pretreatment of BDD Electrodes.** The surface termination of BDD affects the electrochemical behavior of the electrode. Charge transfer is enhanced when working with hydrogen-terminated surfaces. Oxygen-terminated sites are formed during oxidation at positive potential in the presence of oxygen. Reversion to an H-terminated surface is possible by cathodic pretreatment at high negative potentials in an acidic environment.<sup>10</sup>

Deterioration of BDD-electrode performance was observed after repeated peptide oxidation over a period of several days by a progressive decrease of oxidation yields to 20–30%. Figure 2

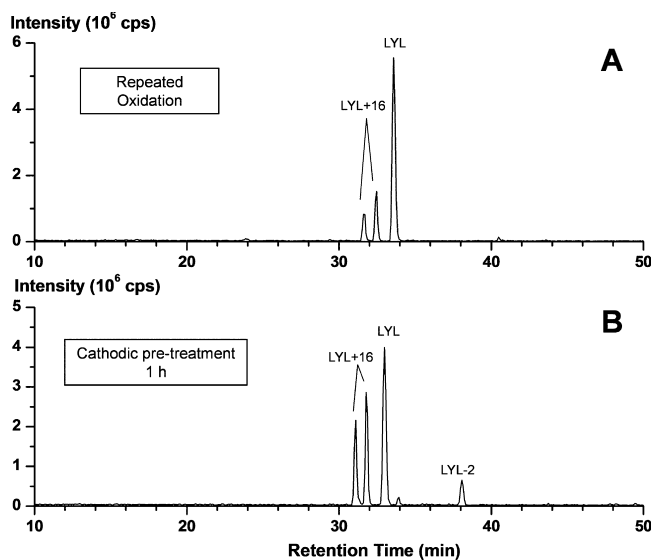


**Figure 2.** Influence of cathodic pretreatment on the performance of a BDD electrode for the oxidation of 5  $\mu\text{M}$  LYL in  $\text{H}_2\text{O}/\text{CH}_3\text{CN}/\text{HCOOH}$  (89:10:1) at a flow rate of 5  $\mu\text{L}/\text{min}$  at 2000 mV. Base peak chromatograms of the reaction products (A) prior to and (B) after cathodic pretreatment at a constant potential of  $-3000$  mV for 1 h in the presence of 0.5 M sulfuric acid.

illustrates the conversion of the tripeptide LYL prior to and after 1 h of cathodic pretreatment. Electrode pretreatment was performed by applying a constant potential of  $-3000$  mV in the presence of 0.5 M sulfuric acid and resulted in oxidation yields of 60–70%, which are comparable to the values observed originally. This is attributed to the replacement of O-terminated by H-terminated sites. Cathodic pretreatment has to be carried out regularly in order to ensure reliable and reproducible results for the present set of peptides. No significant drop in performance was observed after one day of oxidation of either LYL or blank solution (Figure S2 in SI) indicating that peptide adsorption is very low and that daily regeneration the electrode is sufficient for reproducible results.

**Peptide Cleavage on a Thin-Layer GC Electrode.** For comparison with the BDD electrode, electrochemical oxidation was performed with a GC electrode of identical size (8 mm diameter). The tripeptide LYL was used to determine the optimal potential for maximum conversion by ramping the oxidation potential in 100 mV increments and following product distribution by LC–MS analysis. All experiments were performed at 5  $\mu\text{M}$  peptide concentration with flow rates in the

low  $\mu\text{L}/\text{min}$  range. Oxidation of LYL started at 1000 mV vs  $\text{Pd}/\text{H}_2$  but with a low oxidation yield. Maximal conversion of 30–40% was reached at a potential of 1500 mV (Figure 3A)

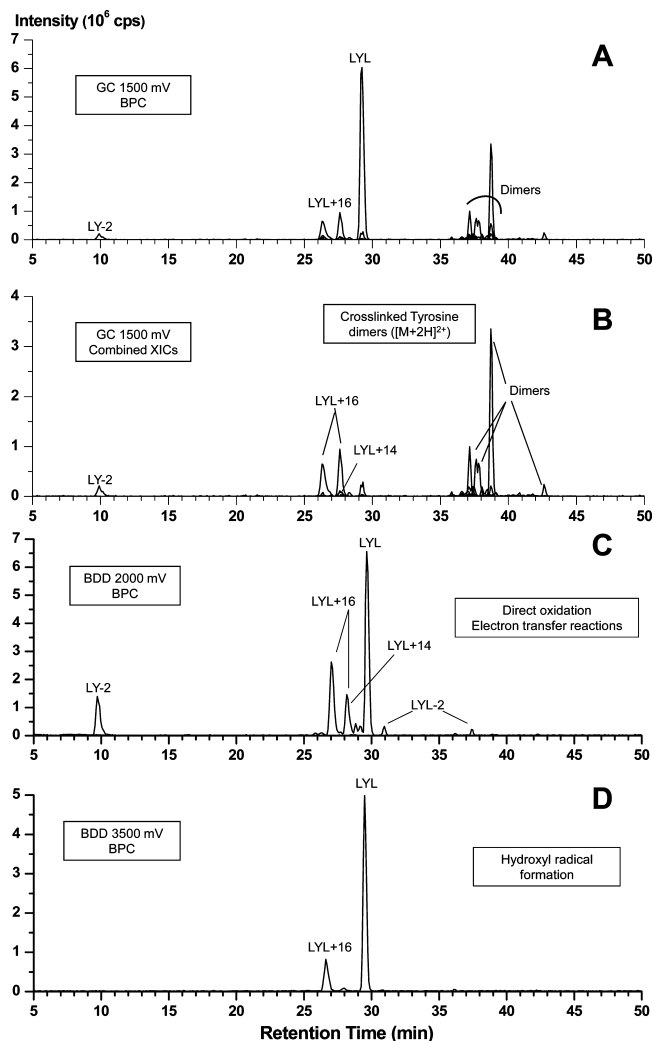


**Figure 3.** LC–MS chromatograms of reaction products obtained after electrochemical oxidation of 5  $\mu\text{M}$  LYL in  $\text{H}_2\text{O}/\text{CH}_3\text{CN}/\text{HCOOH}$  (89:10:1) at a flow rate of 5  $\mu\text{L}/\text{min}$ . (A) Base peak chromatogram and (B) combined extracted ion chromatograms (XICs) of the main oxidation and cleavage products obtained on a GC electrode at 1500 mV. Base peak chromatogram obtained on a BDD electrode at (C) 2000 mV and (D) 3500 mV. Note that there is no cleavage at 3500 mV.

which preceded a gradual decrease of peptide signal when increasing the potential above 1500 mV. Cyclic voltammetry experiments (Figure S1 of SI) confirmed the onset of LYL oxidation at 1000 mV (Figure S1, panel C in SI) and revealed that water oxidation was initiated at 1500 mV (Figure S1, panel A in SI) which is in agreement with the optimal potential deduced from LC–MS experiments. The range of oxidation and cleavage products detected on the GC electrode in a thin-layer cell is detailed in Figure 3B and is in accordance with the range of products obtained in previous work performed with porous graphite electrodes (ESA 5021 cell).<sup>19</sup> However, the amount of products was much higher in the coulometric ESA cell due to the much larger surface area of the porous graphite electrode (more than 50 times the area of the flat GC

electrode). Dimers formed by Tyr cross-linking reactions are the most abundant oxidation products of the tripeptide LYL on GC, suggesting strong adsorption of the peptide to the working electrode surface. Dimerization of and cross-linking within Tyr-containing peptides and proteins<sup>44,45</sup> readily occurs at the surface of carbon electrodes due to strong adsorption of the phenolic ring.<sup>23</sup> This constitutes a major drawback of GC electrodes, since dimers are formed at the expense of other oxidation products, notably cleavage products.

#### Peptide Cleavage on a Thin-Layer BDD Electrode.

Since formation of hydroxyl radicals on the BDD electrode was observed at a potential of 2500 mV, we choose a potential of 2000 mV as the upper limit for evaluating BDD for the electrochemical oxidation and cleavage of peptides by direct electron transfer.

Hydrodynamic voltammetry performed by ramping the potential in 100 mV increments and following the product distribution by LC–MS showed that oxidation of LYL on BDD was initiated at 1300 mV with a conversion of around 5% and no detectable cleavage products. Both oxidation and cleavage yields increased with higher potentials, and maximum conversion of 50% was obtained at 2000 mV. Cyclic voltammetry experiments performed on BDD (Figure S1 in SI) confirmed the results obtained by LC–MS, i.e. onset of peptide oxidation at 1300 mV (Figure S1, panel D in SI) and water oxidation at potentials greater than 2000 mV (Figure S1, panel B in SI). The cleavage and noncleavage oxidation products are presented in Figure 3C and correspond closely to those obtained on a porous graphite electrode as previously described.<sup>17,19</sup> Since complete conversion can be reached with peptide concentrations of up to 50  $\mu\text{M}$  on the porous graphite electrode, BDD electrodes with larger surface areas are needed to reach similar conversion levels.

Two main differences were observed between BDD and the pure carbon electrodes. First, there is no dimer formation on BDD while this is a significant reaction pathway when working with carbon electrodes as reported above for the oxidation of LYL with a GC disk electrode and in previous work with a porous graphite electrode in a coulometric cell.<sup>19</sup> Dimer formation likely occurs on the electrode surface due to the high local concentration of adsorbed LYL. The observation that LYL does not dimerize even at high positive potentials indicates that adsorption to BDD electrodes is much lower. We therefore used the extent of Tyr-mediated dimer formation as an indirect measure of peptide adsorption. Second, when potentials greater than 2000 mV were applied, a progressive decrease of the cleavage yield with a concomitant increase of the M+16 hydroxylated products was observed (see Figure 3D for the reaction products observed at 3500 mV). This observation confirms the oxidation pathway by reaction with hydroxyl radicals at very positive potentials on the BDD electrode and shows that this goes at the expense of cleavage product formation.

**Electrochemical Oxidation of Larger Peptides.** Two decapeptides, angiotensin I and adrenocorticotrophic hormone (ACTH) 1-10, were analyzed to compare BDD and GC electrodes with larger peptides in view of the adsorption issues encountered previously on porous graphite electrodes.<sup>17,18</sup>

Angiotensin I (DRVYIHPFHL) contains a single Tyr residue that is amenable to direct electrochemical oxidation. Earlier experiments with porous graphite electrodes<sup>17</sup> showed that it is possible to cleave this peptide C-terminal to the Tyr residue but with poor reproducibility, presumably due to adsorption of the

peptide at the electrode surface. Angiotensin I was successfully oxidized at the BDD electrode in the thin layer cell with a conversion yield of 20–30% (Figure 4A), which was lower than

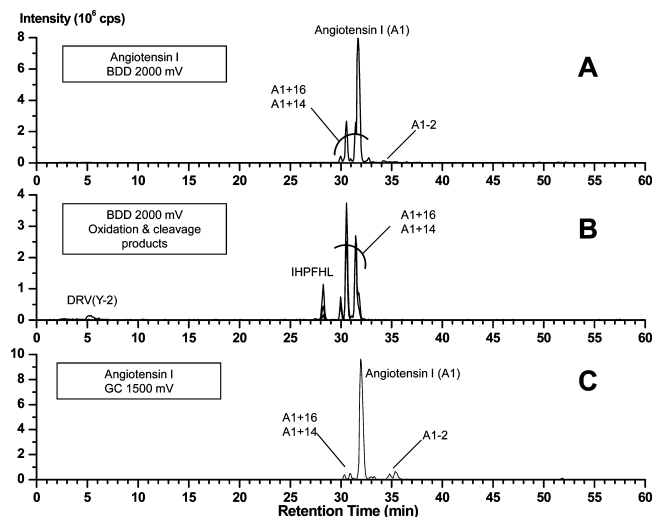


**Figure 4.** LC–MS chromatograms of reaction products obtained after oxidation of 5  $\mu\text{M}$  angiotensin I (DRVYIHPFHL) in  $\text{H}_2\text{O}/\text{CH}_3\text{CN}/\text{HCOOH}$  (89:10:1) at a flow rate of 5  $\mu\text{L}/\text{min}$  at (A) 2000 mV on BDD and (C) 1500 mV on GC electrodes. (B) Extracted ion chromatograms (XICs) of the main oxidation and cleavage products obtained on the BDD electrode at 2000 mV.

for LYL. Lower conversion yields for larger peptides may be explained by their lower diffusion rates. While oxidation yielded mainly noncleavage products, listed as A1–2, A1+14, A1+16 in panels A and B of Figure 4, the cleavage products DRVY-2 and IHPFHL were clearly detectable (Figure 4B). When the performance of the BDD and the GC electrodes in the thin-layer cell was compared with respect to the conversion of angiotensin I (Figure 4C), a significantly lower yield was observed with the GC electrode. This lower efficiency may again be explained by adsorption on the surface of the GC electrode leading to a low recovery of oxidation products. Dimer formation was, however, not detected, possibly due to the low oxidation yields or to adsorption of the dimer on the electrode surface.

The second peptide we evaluated was ACTH 1-10 (SYSMEHFRWG). This peptide has been tested earlier with porous graphite electrode-containing coulometric cells, but no products were detected, presumably due to very strong adsorption on the porous graphite electrode.<sup>18</sup> It was thus of interest to determine whether lower adsorption on the BDD electrode would allow identification of oxidation or cleavage products. Another interesting feature of this peptide is that it contains three residues, i.e. Tyr, Met, and Trp, that can be readily oxidized electrochemically by direct electron transfer reactions. This peptide is therefore useful to determine which oxidation pathways occur preferentially, and whether cleavage will occur next to both Tyr and Trp under the same conditions.

Oxidation of ACTH 1-10 at 2000 mV at the BDD working electrode showed noncleavage oxidation products (Figure 5A) containing the expected ACTH-2, ACTH+14, ACTH+16, ACTH+32, ACTH+48 in analogy to those obtained with LYL and LWL.<sup>19</sup> In addition, two out of the three possible cleavage products were detected as shown in Figure 5B, namely the C-terminal peptide formed by cleavage next to Tyr

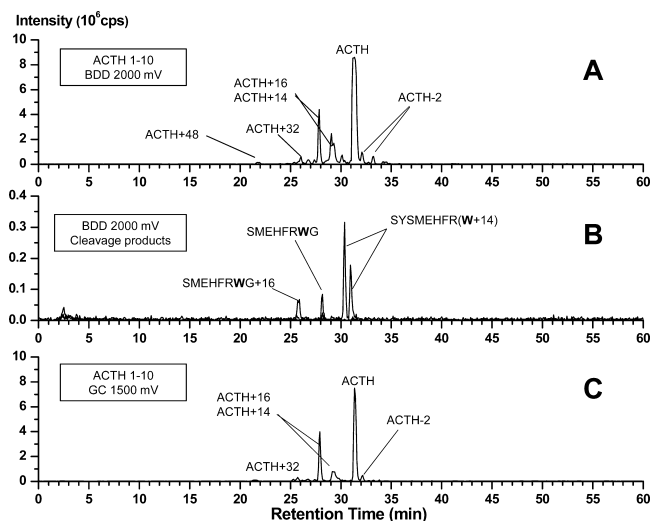


**Figure 5.** LC–MS chromatograms of reaction products obtained after oxidation of 5  $\mu$ M ACTH 1-10 (SYSMEHFRWG) in  $\text{H}_2\text{O}/\text{CH}_3\text{CN}/\text{HCOOH}$  (89:10:1) at a flow rate of 5  $\mu\text{L}/\text{min}$  at (A) 2000 mV on BDD and (C) 1500 mV on GC electrodes. (B) Extracted ion chromatograms (XICs) of the cleavage products obtained on the BDD electrode at 2000 mV.

(SMEHFRWG) and the N-terminal peptide formed by cleavage next to Trp (SYSMEHFRW+14). The corresponding small cleavage products (SY-2 and G) were not detected, probably due to poor retention on the reversed-phase column during LC–MS analysis. The higher intensity of the Trp cleavage product suggests that this reaction is favored under these conditions. Interestingly, the Trp cleavage product eluted in two peaks, suggesting the formation of isomers (Figure 5B). This has not been reported in our earlier study of Trp-containing tripeptides (performed on porous carbon electrodes).<sup>19</sup> This might indicate the formation of conformational isomers that can be detected due to the higher oxidation and cleavage yields obtained on BDD. Conformational isomers have also been observed after chemical labeling of Trp-containing peptides after electrochemical cleavage.<sup>46</sup> Modification of oxidizable amino acids present in the cleavage products of ACTH 1-10 did not always take place. S-oxidation of Met within the N-terminal peptide SMEHFRW+14 was not detected. On the other hand, oxidation within the C-terminal peptide obtained after cleavage next to Tyr (SMEHFRWG+16) was observed, most likely due to hydroxylation of Trp. The thin-layer cell containing a GC electrode of identical dimensions resulted in lower conversion and cleavage yields possibly due to peptide adsorption as indicated by dark deposits on the GC electrode (Figure 5C).

## CONCLUSIONS

Boron-doped diamond (BDD) was investigated as electrode material in comparison to the more commonly used glassy carbon (GC) electrodes with respect to the electrochemical oxidation and cleavage of peptides. Lower adsorption of peptides on BDD was indicated by the absence of Tyr dimer formation at the electrode surface, even at elevated potentials as opposed to high amounts of Tyr dimers on GC. The maximal potential on BDD was limited to 2000 mV vs Pd/ $\text{H}_2$  to prevent hydroxyl radical formation occurring at 2500 mV vs Pd/ $\text{H}_2$ . Cathodic pretreatment of the BDD electrode was shown to be effective in regenerating the electrode surface to ensure

maximal conversion rates and to obtain reliable and reproducible results even after repeated use of the electrode. Investigation of the larger decapeptides angiotensin I and ACTH 1-10 demonstrated the benefit of BDD in comparison to GC in achieving cleavage of the peptide bond C-terminal to Tyr and Trp.

## ASSOCIATED CONTENT

### Supporting Information

This material is available free of charge via the Internet at <http://pubs.acs.org>.

## AUTHOR INFORMATION

### Corresponding Author

\*Tel.: +31 50 363 3338. Fax: +31 50 363 7582. E-mail: r.p.h.bischoff@rug.nl.

### Notes

The authors declare no competing financial interest.

## ACKNOWLEDGMENTS

The Dutch Technology Foundation (STW) is gratefully acknowledged for financial support (Grant 07047). Further financial support was obtained from Astra Zeneca (Mölnådal, Sweden) and Organon, (Oss, The Netherlands; a former subsidiary of Merck & Co. Inc., Whitehouse Station, NJ, U.S.A.). Electrochemical cells were donated by ESA Inc. (Bedford, MA, U.S.A.) and LC equipment by LC-Packings (Amsterdam, The Netherlands; now both part of Thermo Scientific, Sunnyvale, CA, U.S.A.).

## REFERENCES

- McCreery, R. L. *Chem. Rev.* **2008**, *108*, 2646–2687.
- Luong, J. H. T.; Male, K. B.; Glennon, J. B. *Analyst* **2009**, *134*, 1965–1979.
- Pleskov, Y. V.; Sakharova, A. Y.; Krotova, M. D. *J. Electroanal. Chem.* **1987**, *228*, 19–27.
- Kraft, A. *Int. J. Electrochem. Sci.* **2007**, *2*, 355–385.
- Xu, G.; Chance, M. R. *Chem. Rev.* **2007**, *107*, 3514–3543.
- Pleskov, Y. V. *Russ. J. Electrochem.* **2002**, *38*, 1275–1291.
- Swain, G. M. In *Electroanalytical Chemistry*; Bard, A. J., Rubinstein, I., Eds.; Marcel Dekker: New York, 2004; Vol. 22.
- Pecková, K.; Musilová, J.; Barek, J. *Crit. Rev. Anal. Chem.* **2009**, *39*, 148–172.
- Granger, M. C.; Witek, M.; Xu, J.; Wang, J.; Hupert, M.; Hanks, A.; Koppang, M. D.; Butler, J. E.; Lucazeau, G.; Mermoux, M.; Strojek, J. W.; Swain, G. M. *Anal. Chem.* **2000**, *72*, 3793–3804.
- Salazar-Banda, G. R.; Andrade, L. S.; Nascente, P. A. P.; Pizani, P. S.; Rocha-Filho, R. C.; Avaca, L. A. *Electrochim. Acta* **2006**, *51*, 4612–4619.
- Suffredini, H. B.; Pedrosa, V. A.; Codognoto, L.; Machado, S. A. S.; Rocha-Filho, R. C.; Avaca, L. A. *Electrochim. Acta* **2004**, *49*, 4021–4026.
- Chiku, M.; Ivandini, T. A.; Kamiya, A.; Fujishima, A.; Einaga, Y. *J. Electroanal. Chem.* **2008**, *612*, 201–207.
- McClintock, C.; Kertesz, V.; Hettich, R. L. *Anal. Chem.* **2008**, *80*, 3304–3317.
- Sumi, T.; Saitoh, T.; Natsui, K.; Yamamoto, T.; Atobe, M.; Einaga, Y.; Nishiyama, S. *Angew. Chem., Int. Ed.* **2012**, *51*, 5443–5446.
- Iniesta, J.; Michaud, P. A.; Panizza, M.; Comninellis, C. *Electrochem. Commun.* **2001**, *3*, 346–351.
- Fardel, R.; Griesbach, U.; Pütter, H.; Comninellis, C. *J. Appl. Electrochem.* **2006**, *36*, 249–253.
- Permentier, H. P.; Jurva, U.; Barroso, B.; Bruins, A. P. *Rapid Commun. Mass Spectrom.* **2003**, *17*, 1585–1592.

- (18) Permentier, H. P.; Bruins, A. P. *J. Am. Soc. Mass Spectrom* **2004**, *15*, 1707–1716.
- (19) Roeser, J.; Permentier, H. P.; Bruins, A. P.; Bischoff, R. *Anal. Chem.* **2010**, *82*, 7556–7565.
- (20) Eickhoff, H.; Jung, G.; Rieker, A. *Tetrahedron* **2001**, *57*, 353–364.
- (21) Giulivi, C.; Traaseth, N. J.; Davies, K. J. A. *Amino Acids* **2003**, *25*, 227–232.
- (22) Zhang, M.; Mullens, C.; Gorski, W. *Anal. Chem.* **2005**, *77*, 6396–6401.
- (23) Lund, H.; Hammerich, O. *Organic Electrochemistry*; Marcel Dekker: New York, 2001.
- (24) Foord, J. S.; Chatterjee, A. *Phys. Status Solidi A* **2005**, *202*, 2110–2115.
- (25) Zhao, G.; Qi, Y.; Tian, Y. *Electroanalysis* **2006**, *18*, 830–834.
- (26) Szunerits, S.; Coffinier, Y.; Galopin, E.; Brenner, J.; Boukherroub, R. *Electrochem. Commun.* **2010**, *12*, 438–441.
- (27) Spataru, N.; Sarada, B. V.; Popa, E.; Tryk, D. A.; Fujishima, A. *Anal. Chem.* **2001**, *73*, 514–519.
- (28) Terashima, C.; Rao, T. N.; Sarada, B. V.; Fujishima, A. *Chem. Lett.* **2003**, *32*, 136–137.
- (29) Terashima, C.; Rao, T. N.; Sarada, B. V.; Kubota, Y.; Fujishima, A. *Anal. Chem.* **2003**, *75*, 1564–1572.
- (30) Chailapakul, O.; Aksharanandana, P.; Frelink, T.; Einaga, Y.; Fujishima, A. *Sens. Actuators B* **2001**, *80*, 193–201.
- (31) Ivandini, T. A.; Sarada, B. V.; Terashima, C.; Rao, T. N.; Tryk, D. A.; Ishiguro, H.; Kubota, Y.; Fujishima, A. *J. Chromatogr., B* **2003**, *791*, 63–72.
- (32) Chiku, M.; Nakamura, J.; Fujishima, A.; Einaga, Y. *Anal. Chem.* **2008**, *80*, 5783–5787.
- (33) Chiku, M.; Horisawa, K.; Doi, N.; Yanagawa, H.; Einaga, Y. *Biosens. Bioelectron.* **2010**, *26*, 235–240.
- (34) Iniesta, J.; Esclapez-Vicente, M. D.; Heptinstall, J.; Walton, D. J.; Peterson, I. R.; Mikhailov, V. A.; Cooper, H. J. *Enzyme Microb. Technol.* **2010**, *46*, 472–478.
- (35) Zhang, J. D.; Oyama, M. *Microchem. J.* **2004**, *78*, 217–222.
- (36) McEvoy, J. P.; Foord, F. S. *Electrochim. Acta* **2005**, *50*, 2933–2941.
- (37) Marken, F.; Paddon, C. A.; Asogan, D. *Electrochem. Commun.* **2002**, *4*, 62–66.
- (38) Haymond, S.; Babcock, G. T.; Swain, G. M. *J. Am. Chem. Soc.* **2002**, *124*, 10634–10635.
- (39) Shin, D.; Tryk, D. A.; Fujishima, A.; Merkoçi, A.; Wang, J. *Electroanalysis* **2005**, *17*, 305–311.
- (40) Witek, M.; Swain, G. M. *Anal. Chim. Acta* **2001**, *440*, 119–129.
- (41) Rao, T. N.; Yagi, I.; Miwa, T.; Tryk, D. A.; Fujishima, A. *Anal. Chem.* **1999**, *71*, 2506–2511.
- (42) Trouillon, R.; O'Hare, D. *Electrochim. Acta* **2010**, *55*, 6586–6595.
- (43) Stadtman, E. R.; Levine, R. L. *Amino Acids* **2003**, *25*, 207–218.
- (44) Burzio, L. A.; Waite, J. H. *Protein Sci.* **2001**, *10*, 735–740.
- (45) Michon, T.; Chenu, M.; Kellershon, N.; Desmadril, M.; Gueguen, J. *Biochemistry* **1997**, *36*, 8504–8513.
- (46) Roeser, J.; Alting, N. F. A.; Permentier, H. P.; Bruins, A. P.; Bischoff, R. *Rapid Commun. Mass Spectrom.* **2013**, *27*, 546–552.